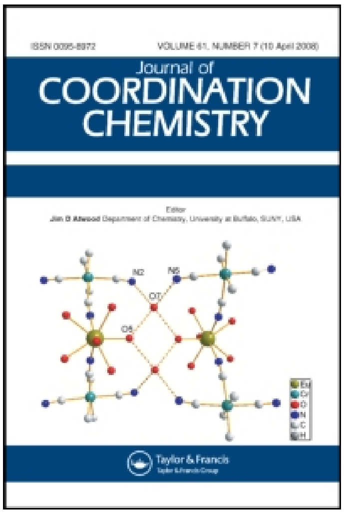

Journal of Coordination Chemistry
Publication details, including instructions for authors and subscription information:
http://www.informaworld.com/smpp/title~content=t713455674

Structures and theoretical studies of three copper(II) complexes containing 2,2'-dipyridylamine and acrylato or methylacrylato ligands

Ping Liu[a]; Cui-Juan Wang[a]; Yao-Yu Wang[a]; Wen-Long Qin[a]; Rui Sun[a]; Dong-Sheng Li[a]; Qi-Zhen Shi[a]
[a] Department of Chemistry, Shaanxi Key Laboratory of Physico-inorganic Chemistry, Northwest University, Xi'an, Shaanxi 710069, China

To cite this Article Liu, Ping , Wang, Cui-Juan , Wang, Yao-Yu , Qin, Wen-Long , Sun, Rui , Li, Dong-Sheng and Shi, Qi-Zhen(2006) 'Structures and theoretical studies of three copper(II) complexes containing 2,2'-dipyridylamine and acrylato or methylacrylato ligands', Journal of Coordination Chemistry, 59: 7, 729 — 741

To link to this Article: DOI: 10.1080/00958970500396243

URL: http://dx.doi.org/10.1080/00958970500396243

Journal of Coordination Chemistry
Vol. 59, No. 7, 10 May 2006, 729–741

Taylor & Francis
Taylor & Francis Group

Structures and theoretical studies of three copper(II) complexes containing 2,2′-dipyridylamine and acrylato or methylacrylato ligands

PING LIU, CUI-JUAN WANG, YAO-YU WANG*, WEN-LONG QIN, RUI SUN, DONG-SHENG LI and QI-ZHEN SHI

Department of Chemistry, Shaanxi Key Laboratory of Physico-inorganic Chemistry,
Northwest University, Xi'an, Shaanxi 710069, China

(*Received 25 February 2005; in final form 28 March 2005*)

A series of new complexes of copper(II): $[Cu(CH_2{=}C(Me)CO_2)_2(dpa)]\cdot H_2O$ (**1**), $[Cu(CH_2{=}CHCO_2)_2(dpa)]\cdot H_2O$ (**2**), $Cu(CH_3CH{=}CHCO_2)_2(dpa)(H_2O)$ (**3**) (dpa = 2,2′-dipyridylamine) have been prepared and characterized by elemental analysis, IR spectra, thermal analysis, density functional theory (DFT) calculations and X-ray structure analysis. The crystal structures of **1** and **2** consist of neutral $[Cu(L)_2(dpa)]$ ($L = CH_2{=}C(Me)CO_2^-$ and $CH_2{=}CHCO_2^-$) units and one lattice water molecule in the unit cell, while in **3** the water molecule is found to coordinate to copper(II). The mononuclear units of **1** and **2** are linked via a similar triple-hydrogen-bonding uncoordinated water molecule into different supramolecular structures, 1D double chains for **1** and a 2D supramolecular network for **2**. A detailed crystal structure analysis of **2** revealed that the presence of the C–H···O and C–H···C hydrogen bonds appear to be responsible for the difference in supramolecular structures differences between **1** and **2**. In **3**, 1D double chains are formed through hydrogen bonds and weak π–π stacking along the *a*-axis. In this context, we addressed the questions concerning the molecular energies, stabilities and atomic charges. The DFT calculation results proved that the water molecules coordinate to copper(II) atoms in complex **3**, while the water molecules in complexes **1** and **2** are free.

Keywords: Copper(II) complexes; DFT calculations; 2,2′-Dipyridylamine; Hydrogen bond; Crystal structure

1. Introduction

The development of supramolecular architectures of inorganic, organic hybrid molecules with various shapes and sizes formed through control and manipulation of weak interaction via non-covalent forces is an exciting area of research that has implications for the rational design of functional materials [1–4]. Self-assembly of suitable molecular components is an efficient way for facile tuning of structural and electronic functions in materials research and in the interpretation of electron/energy transport

---

*Corresponding author. Tel.: +86-29-88303097. Fax: +86-29-88373398. E-mail: wyaoyu@nwu.edu.cn

Journal of Coordination Chemistry
ISSN 0095-8972 print: ISSN 1029-0389 online © 2006 Taylor & Francis
DOI: 10.1080/00958970500396243

in bioactive molecules [4, 5]. 2,2′-Dipyridylamine (dpa) is important in this regard because of its ability to form hydrogen bonded networks through active amine (–NH–) hydrogen [6–9] and to coordinate to metal atoms in a variety of ways [6–13], for example as bidentate ligand through its two pyridyl nitrogen atoms and as a bridging ligand after removal of the amine hydrogen. Additionally, considering the special bioactive and biocatalytic functions of copper(II) carboxylate complexes along with their interesting supramolecular structures, we focused our work on the α,β-unsaturated carboxylate copper(II) and dpa system. We reported 1D chain supramolecular complexes of copper(II) α,β-unsaturated carboxylate $Cu_2(CH_2{=}CHCO_2)_4(H_2O)_2$ in 1999 [14], then in 2000 synthesized 2D network supramolecular complexes of α,β-unsaturated carboxylate with trimethyl phosphate – a copper protein model containing lecithin [15]. In this article, as part of our current research, we have synthesized and characterized three mononuclear $[Cu(CH_2{=}C(Me)CO_2)_2(dpa)]\cdot H_2O$ (**1**), $[Cu(CH_2{=}CHCO_2)_2(dpa)]\cdot H_2O$ (**2**) and $Cu(CH_3CH{=}CHCO_2)_2(dpa)(H_2O)$ (**3**) (dpa = 2,2′-dipyridylamine) complexes, which show self-assembled superstructures via noncovalent interactions in the solid state. The individual units in **1** and **2** have a similar triple-hydrogen-bonding water molecule leading to different supramolecular structures, 1D double chains for **1** and a 2D supramolecular network for **2**. The presence of the C–H···O and C–H···C hydrogen bonds appear to be responsible for the supramolecular structures differences between **1** and **2**. In **3**, the 1D double chains are formed through N–H···O and O–H···O hydrogen bonds and weak π–π stacking along the *a*-axis. Interestingly, though the three α,β-unsaturated carboxylate complexes are similar, the structures of these complexes are different in whether water coordinates to copper. Therefore, DFT calculations were carried out on these three complexes, and the results of theoretical calculations proved the water molecules coordinate to copper(II) atoms in complex **3**, while the water in complexes **1** and **2** are free.

2. Experimental

2.1. *Preparation*

All chemicals were purchased commercially and were used as received. $Cu_2[CH_2{=}C(Me)CO_2]_4(H_2O)_2$, $Cu_2(CH_2{=}CHCO_2)_4(H_2O)_2$ and $Cu_2(CH_3CH{=}CHCO_2)_4(H_2O)_2$ were prepared according to the literature method [14].

2.1.1. $[Cu(CH_2{=}C(Me)CO_2)_2(dpa)]\cdot H_2O$ (1). A methanol solution (10 mL) of dpa (0.38 g, 2 mmol) was added to a solution of $Cu_2[CH_2{=}C(Me)CO_2]_4(H_2O)_2$ (0.50 g, 1 mmol) in the same solvent (10 mL). The mixture was filtered and the green resultant solution was kept in air for slow evaporation. After a few days, blue crystals of **1** were obtained, washed with toluene and dried *in vacuo* over silica gel indicator. The single crystal of **1** suitable for X-ray crystallography is recrystallized from methanol and acetone (1 : 5 v/v). Anal. Calcd for $C_{18}H_{21}CuN_3O_5$(%): C, 51.07; H, 4.97; N, 9.93. Found: C, 51.11; H, 5.00; N, 9.90.

2.1.2. $[Cu(CH_2{=}CHCO_2)_2(dpa)]\cdot H_2O$ (2) and $Cu(CH_3CH{=}CHCO_2)_2(dpa)(H_2O)$ (3). The two complexes were prepared according to the above procedure, using $Cu_2(CH_2{=}CHCO_2)_4(H_2O)_2$ and $Cu_2(CH_3CH{=}CHCO_2)_4(H_2O)_2$ instead of

Table 1. Summary of the crystallographic data for **1**–**3**.

	1	**2**	**3**
Empirical formula	$C_{18}H_{21}CuN_3O_5$	$C_{16}H_{17}CuN_3O_5$	$C_{18}H_{21}CuN_3O_5$
Formula weight	422.92	394.87	422.92
Temperature (T)	293(2)	293(2)	293(2)
Radiation (Å)	Mo-Kα, 0.71073	Mo-Kα, 0.71073	Mo-Kα, 0.71073
Crystal system	Monoclinic	Monoclinic	Monoclinic
Space group	$P2_1/n$	$P2_1/n$	$P2_1/n$
a (Å)	8.3715(9)	14.349(3)	7.1113(7)
b (Å)	15.723(2)	14.486(2)	16.8303(15)
c (Å)	15.541(2)	8.402(2)	15.9850(14)
β (°)	101.478(2)	97.21(2)	91.291(2)
D_{Calcd} (Mg m^{-3})	1.401	1.514	1.469
Crystal size (mm^3)	$0.531 \times 0.314 \times 0.226$	$0.30 \times 0.25 \times 0.21$	$0.38 \times 0.26 \times 0.19$
Crystal colour	Blue	Blue	Blue
Z	4	4	4
V (Å^3)	2004.7	1732.6	1912.7
μ (mm^{-1})	1.122	1.292	1.176
Index ranges	$-11 \le h \le 10$; $-20 \le k \le 19$; $-15 \le l \le 20$	$0 \le h \le 18$; $-18 \le k \le 0$; $-10 \le l \le 10$	$-8 \le h \le 9$; $-22 \le k \le 21$; $-19 \le l \le 21$
Reflections collected	11652	3932	11098
Independent reflections	4348 [R(int) = 0.0780]	3786 [R(int) = 0.0308]	4164 [R(int) = 0.0645]
Refinement method	Full-matrix least-squares on F^2	Full-matrix least-squares on F^2	Full-matrix least-squares on F^2
Absorption correction	Empirical	Psi-scans	Empirical
Final R indices [$I > 2\sigma(I)$]	$R_1 = 0.0478$, $wR_2 = 0.1285$	$R_1 = 0.0374$, $wR_2 = 0.0941$	$R_1 = 0.0398$, $wR_2 = 0.0924$
R indices (all data)	$R_1 = 0.0634$, $wR_2 = 0.1348$	$R_1 = 0.0959$, $wR_2 = 0.1230$	$R_1 = 0.0556$, $wR_2 = 0.0977$
Residual extreme (e Å^{-3})	−0.252, 0.570	−0.462, 0.349	−0.357, 0.327

$Cu_2[CH_2{=}C(Me)CO_2]_4(H_2O)_2$. For **2**, Anal. Calcd for $C_{16}H_{17}CuN_3O_5$(%): C, 48.62; H, 4.31; N, 10.64. Found: C, 48.78; H, 4.25; N, 10.60. For **3**, Anal. Calcd for $C_{18}H_{21}CuN_3O_5$(%): C, 51.07; H, 4.97; N, 9.93. Found: C, 51.01; H, 5.10; N, 10.02.

2.2. *X-ray crystal structure determination*

Data collection for **1** and **3** were performed at 293(2) K on a Bruker SMART APEX CCD-based diffractometer equipped with graphite monochromated Mo-Kα radiation ($\lambda = 0.071073$ nm). Diffraction data for **2** were obtained on a Rigaku AFC7R diffractometer, employing graphite monochromated Mo-Kα radiation ($\lambda = 0.071073$ nm). The structures were solved by direct methods and refined by full-matrix least-squares on F^2 with the SHELXTL program. The non-hydrogen atoms were located with difference Fourier synthesis, and the hydrogen atoms were generated geometrically. Crystallographic data are summarized in table 1, and selected bond distances and bond angles are given in table 2 for **1**–**3**. Hydrogen bonds are displayed in table 3 for **1**–**3**.

2.3. *Physical measurements*

C, H and N elemental analyses were performed on a PE 2400 Elemental analyzer. IR spectra were recorded using KBr pellets with a Bruker EQUINOX 55 spectrometer. UV-Visible spectra were recorded on a PE – Lambda 40 P spectrophotometer.

Table 2. Selected bond distances (Å) and angles (°) for **1**, **2** and **3**.

Complex **1**			
Cu–O3	1.966(2)	Cu–N1	1.973(2)
Cu–O1	1.978(2)	Cu–N2	1.978(2)
O3–Cu–N1	153.97(10)	O3–Cu–N2	93.13(10)
O3–Cu–O1	92.13(9)	N1–Cu–N2	92.68(9)
N1–Cu–O1	93.76(9)	O1–Cu–N2	153.79(9)
Complex **2**			
Cu–O2	1.987(3)	Cu–N1	1.972(3)
Cu–O4	1.978(2)	Cu–N3	1.977(3)
O2–Cu–O4	92.9(1)	O4–Cu–N1	151.4(1)
O2–Cu–N1	92.8(1)	O4–Cu–N3	95.3(1)
O2–Cu–N3	152.6(1)	N1–Cu–N3	92.3(1)
Complex **3**			
Cu–O3	1.9436(2)	Cu–N1	1.9956(2)
Cu–O1	1.9948(2)	Cu–N3	2.022(2)
Cu–O5	2.211(3)		
O3–Cu–N1	175.66(8)	O3–Cu–O1	86.98(8)
N1–Cu–O1	89.20(7)	O3–Cu–N3	92.38(8)
N1–Cu–N3	90.31(7)	O1–Cu–N3	156.82(8)
O5–Cu–O3	93.13(9)	O5–Cu–O1	96.85(12)
O5–Cu–N1	89.39(9)	O5–Cu–N3	106.32(11)

Table 3. Hydrogen bonds for **1**–**3**.

D–H···A	d(D–H)	d(H···A)	d(D···A)	∠(DHA)
Complex **1**				
O5–H21···O4A	0.890(18)	1.94(2)	2.787(3)	158(3)
O5–H20···O2	0.914(19)	1.81(2)	2.701(4)	166(4)
N3–H19···O5B	0.86	1.99	2.837(3)	169.8
A: $x-1$, y, z; B: $-x+1$, $-y$, $-z+1$				
Complex **2**				
O5–H16···O1	0.921(19)	1.88(3)	2.758(5)	160(5)
N2–H11···O5A	0.80(4)	2.00(4)	2.795(5)	170(4)
O5–H17···O3B	0.91(2)	1.92(3)	2.779(5)	159(6)
C2B–H1B···C11	0.965(1)	2.841(3)	3.368(4)	115.45
C3B–H3B···O3	0.991(1)	0.2722(3)	3.488(4)	134.41
C2B–H1B···O3	0.965(1)	3.0604(4)	3.556(4)	113.71
A: $-x+3/2$, $y+1/2$, $-z+1/2$; B: x, y, $z-1$				
Complex **3**				
O5–H21···O2A	0.833(18)	1.908(19)	2.732(3)	170(3)
N2–H9···O2B	0.806(15)	2.002(16)	2.805(3)	175(2)
O5–H20···O4	0.868(19)	1.78(3)	2.584(3)	153(4)
A: $x+1$, y, z; B: $-x$, $-y+1$, $-z+1$				

Differential thermogravimetric analyses (TGA) and differential scanning calorimetry (DSC) were performed on a Netzsch STA 449C microanalyzer under flowing air with a heating rate of $10^{\circ}\mathrm{C\,min^{-1}}$.

2.4. *Computational details*

The quantum chemical calculations have been performed with Density Functional Theory (DFT) at the B3LYP level using Gaussian 03 program suite. We employed the 6-31G(d) basis set for H, C, N and O, and the LANL2DZ effective core potential (ECP) set of Hay and Wadt for Cu [16]. Geometry optimization was performed for each complex, and the attainment of energy minimum was verified by calculating the vibrational frequencies that result in absence of imaginary eigenvalues. After calculations, relative energies of the three complexes given include zero-point corrections (ZEP), $E_{\text{complex}\,\mathbf{1}} = -1434.22$ (Hartree), $E_{\text{complex}\,\mathbf{2}} = -1279.50$ (Hartree), $E_{\text{complex}\,\mathbf{3}} = -1434.46$ (Hartree).

3. Results and discussion

3.1. *Crystal structure*

The ORTEP diagrams of complexes **1**–**3** are shown in figures 1–3, respectively. In the crystal structure of **1**, there is one copper(II) atom, two carboxylate ligands, one dpa and one lattice water. Each copper(II) atom in **1** is coordinated by two oxygen atoms from two monodentate α-methacrylate ligands (Cu1–O1 1.978(2) and Cu1–O3 1.966(2) Å) and two nitrogen atoms from a chelating dpa ligand (Cu1–N1 1.973(2) and Cu1–N3 1.978(2) Å) to furnish a distorted square-planar geometry (figure 1). The pendant carboxy oxygen atoms have weak bonding interactions with the copper(II) atom at axial sites (Cu1–O2 2.467(2), Cu1–O4 2.589(2) Å) due to the Jahn–Teller effect. The dpa ligand is slightly folded, as the value of the dihedral angle between the planar pyridine rings is 7.190(2)°, smaller than that of free dpa (23°). The Cu1–O(water) bond length is 3.955(3) Å, which is great longer than that of

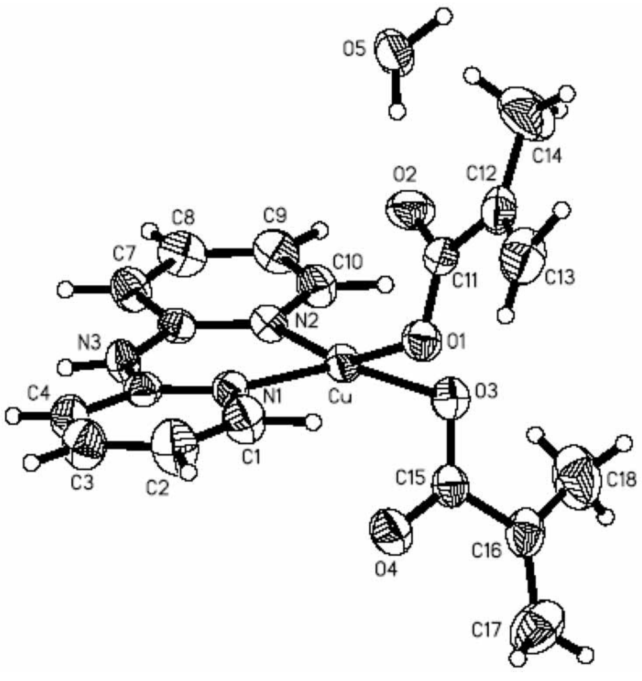

Figure 1. The molecular structure of **1**. The thermal ellipsoids are drawn at the 30% probability level.

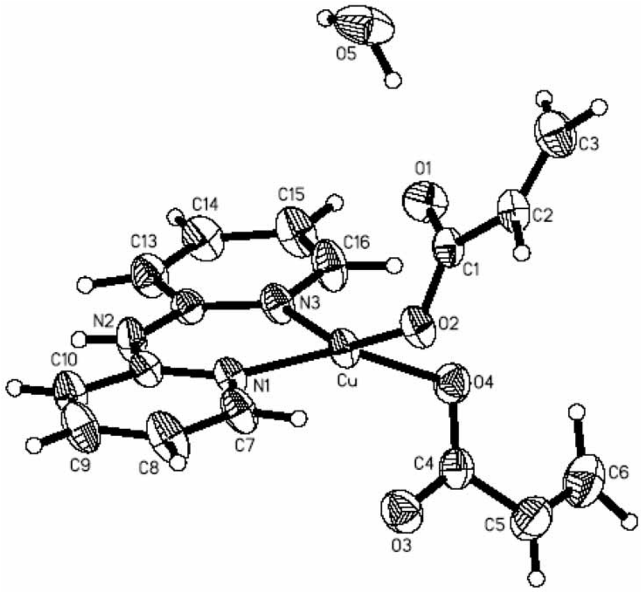

Figure 2. The molecular structure of **2**. The thermal ellipsoids are drawn at the 30% probability level.

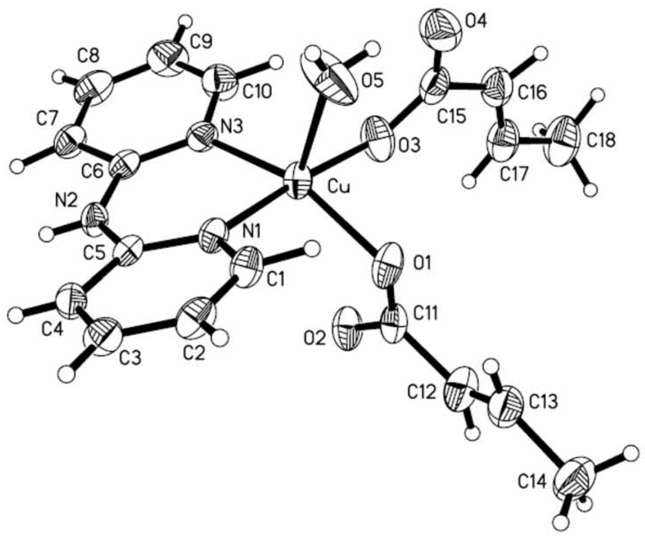

Figure 3. The molecular structure of **3**. The thermal ellipsoids are drawn at the 30% probability level.

Cu1–O(carboxyl), indicating water is free in the crystal lattice. However, from our previous investigations, the water of $Cu(CH_2{=}C(Me)CO_2)_2(bipy)(H_2O)$ (bipy = 2,2′-bipyridine) coordinates to copper(II) (the Cu1–O(water) is 2.301(2) Å), and the copper(II) atoms are square-pyramidal [17]. Recently, complex $[Cu(ndc)(dpa)] \cdot H_2O$ (ndc = 1,4-naphthalenedicarboxylate) was reported to be composed of a copper centered dimer where the copper(II) atoms are square-pyramidal [11].

When acrylate, a α,β-unsaturated carboxylate ligand of smaller size, was used instead of α-methacrylate, analogous neutral molecules are formed (**2**, figure 2). Similar to **1**, the copper(II) atom in 2 is also primarily coordinated by two oxygen atoms from two monodentate acrylate ligands (Cu1–O1 1.978(2) and Cu1–O3 1.966(2) Å) and two nitrogen atoms from a chelating dpa ligand (Cu1–N1 1.973(2) and Cu1–N3 1.978(2) Å) to furnish a distorted square-planar coordination, the Cu1–O1 (2.505(3) Å) and Cu1–O3 (2.566(3) Å) distances show some weak interactions between the copper center and the carboxy oxygen atoms at axial sites. Like **1**, the water molecular is free in the crystal lattice with the distance of Cu–O(water) 4.399(7) Å. The dihedral angle between the planar pyridine rings of dpa is 4.426(5)°, which is smaller than that of **1**.

For complex **3**, the copper(II) atom is primarily ligated by two oxygen atoms from two monodentate crotonate ligands (Cu1–O1 1.995(2) and Cu1–O3 1.944(2) Å) and two nitrogen atoms from a chelating dpa ligand (Cu1–N1 1.996(2) and Cu1–N3 2.022(2) Å) to furnish a distorted square-planar coordination, an aqua oxygen atom (Cu1–O5W 2.211(3) Å) occupies an apical position and Cu1–O2 (2.835(2) Å) distances show some weak interactions between the copper center and the carboxy oxygen atoms at the axial sites (figure 3). The value of the bond length of Cu1–O5W is significantly shorter than that of Cu–O(water) of **1** and **2**, and similar to the length range of Cu–O(carboxyl) and shorter than that of $Cu(CH_2{=}C(Me)CO_2)_2(bipy)(H_2O)$ (the Cu–O(water) is 2.301(3) Å) [17], indicating coordinated water. The dihedral angle between the planar pyridine rings of dpa is 12.614 (6)°, larger than that of **1** and **2**.

The significant difference among the three complexes is the number of lattice water molecules, the arrangement of the neutral mononuclear units and the hydrogen-bonding patterns. Both **1** and **2** contain one lattice water molecule in the unit cell. As indicated in figures 4 and 6, each mononuclear unit of **1** and **2** affords one hydrogen-bond donor (N–H) and two hydrogen bond acceptors (O), and each water molecule has one hydrogen-bond acceptor and two hydrogen-bond donors. However, the structures of **1** and **2** significantly differ in the arrangement of the neutral mononuclear units. In **1**, the neutral mononuclear units are linked via a triple-hydrogen-bonding water molecule to form 1D columnar double chains. As show in figure 4, the lattice water molecules are hydrogen bonding to two adjacent carboxyl oxygen atoms of different units (2.701(4), 2.787(3) Å for O5···O2, O5···O4A respectively) and one adjacent amido nitrogen atom of the third unit (2.837(3) Å

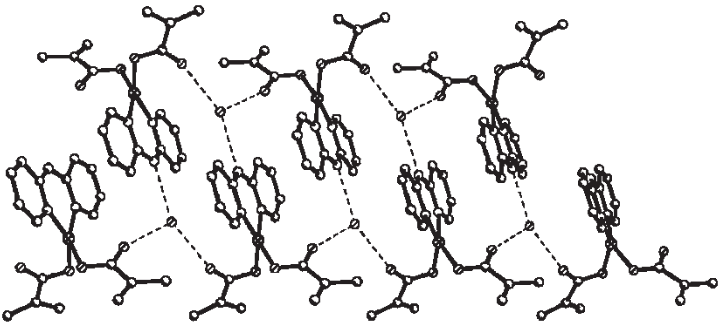

Figure 4. One-dimensional double chains formed through strong hydrogen bonding in complex **1**. Hydrogen atoms are omitted for clarity.

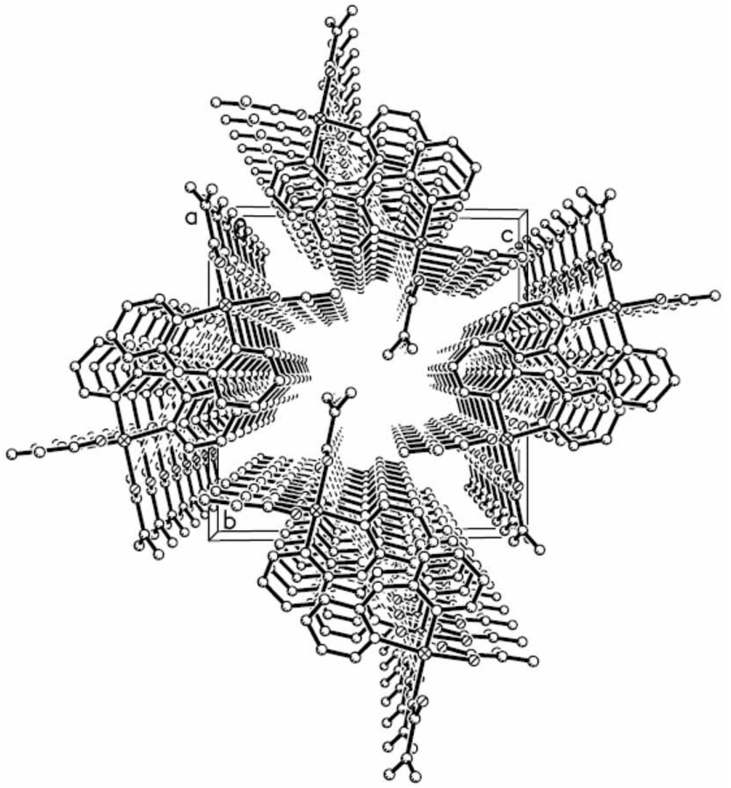

Figure 5. Crystal packing diagram of complex **1** viewed down *a*-axis. Hydrogen atoms are omitted for clarity.

for N3···O5B) (table 3). It can be seen that the plane of the dpa ring of one unit is located *trans* to the other adjacent units. The hydrogen bond contributes much to the stabilization of the lattice. As can been seen from figure 5, every four adjacent columnar double chains stack to form an interesting cavity in the supramolecular structure.

The neutral mononuclear units in **2** are linked via a triple-hydrogen-bonding water molecule to form 2D network (figure 6). The lattice water molecules are hydrogen-bonding to two adjacent carboxyl oxygen atoms of different units (2.758(5), 2.779(5) Å for O5···O1, O5···O3B respectively) and one adjacent amido nitrogen atom of the third unit (2.795(5) Å for N2···O5A) (table 3). Significantly different from **1**, the plane of the dpa ring of one unit is located *cis* to other adjacent units in the network. Interestingly, detailed crystal structure analysis of **2** revealed that the hydrogen bond appears to be responsible for the significant supramolecular structural differences between these two complexes. Because the smaller acrylate group leads to less steric hindrance, an acrylate group of one unit enters the void space between two dpa ligands of the adjacent units. The ethenyl carbon (C2B) of an acrylate group is hydrogen-bonded to the dpa carbon atoms of adjacent unit (3.368(4) Å for C2B···C11), and the ethenyl carbon (C2B and C3B) of an acrylate group are hydrogen bonded to the carboxyl oxygen atom (O3) of adjacent unit with

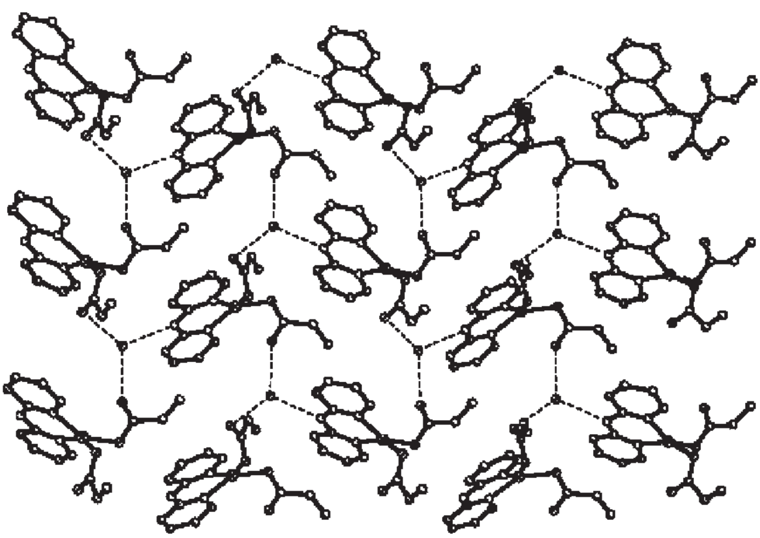

Figure 6. Two-dimensional network structures of complex **2**. Hydrogen atoms are omitted for clarity.

distances of 3.556(4) and 3.488(4) Å, respectively (table 3). There are no π–π stacking interaction in the molecular structures of **1** and **2**.

Compared with **1** and **2**, no free water molecule of **3** is involved in the unit cell. Each mononuclear unit of **3** has two hydrogen-bond donors (N–H and O(water)–H) and one hydrogen bond acceptor (O(carboxyl)). The oxygen atoms (O2) of one crotonate group are simultaneously strongly hydrogen-bonded to the amido nitrogen atom N2 of dpa and the aqua oxygen atom O5 of the adjacent units with distances of 2.732(3) and 2.805(3) Å (table 3), respectively. As a result, 1D double chains are formed through hydrogen bonding (figure 7). Furthermore, the 1D double chain is strengthened by face-to-face weak π–π interactions (C_g(py)$\cdots C_g$(py) 3.862(0) and 4.190(2) Å). Different from **1**, the 1D chain in **3** is formed by strong hydrogen bonds and weak π–π interaction. Similar to **1**, every four adjacent columnar double chains in **3** stack to form an interesting cavity (figure 8).

3.2. *IR spectra*

In the IR spectra, all three complexes show strong bands corresponding to ν_{as}(COO) and ν_s(COO) at 1555 and 1358 cm^{-1} for **1**, 1553 and 1355 cm^{-1} for **2**, and 1584 and 1385 cm^{-1} for **3**. The $\Delta\nu$ of the three complexes are 197, 198 and 199cm^{-1}, larger than the corresponding values for $CH_2{=}CHCO_2Na$, $CH_2{=}C(Me)CO_2Na$ and $CH_3CH_2{=}CHCO_2Na$, indicating that the α,β-unsaturated carboxylate groups behave as monodentate ligands in the complexes [18]. The NH stretches of dpa of **1**–**3** (3395, 3455, and 3450 cm^{-1} shift towards higher wavenumbers indicating coordination [19].

3.3. *Thermal analysis*

To study the thermal stability of complexes **1**–**3**, thermogravimetric analyses and differential scanning calorimetry (TGA and DSC) were performed. The TG curves showed the first stage of weight loss from 80 to 110°C in **1** (70–90°C for **2** and

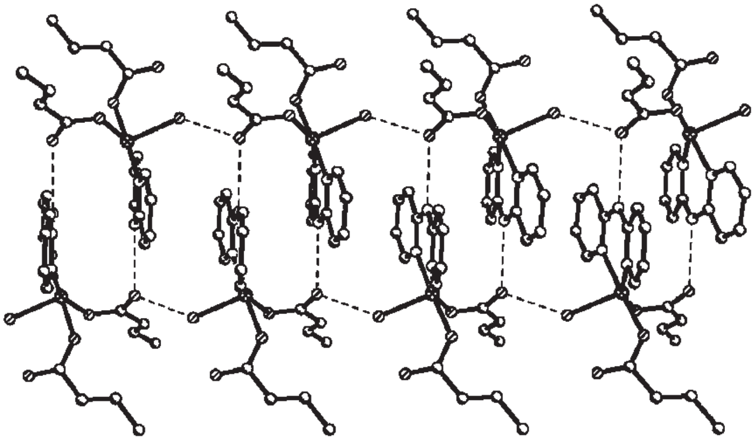

Figure 7. One-dimensional double chains formed through strong hydrogen bonding in complex **3**. Hydrogen atoms are omitted for clarity.

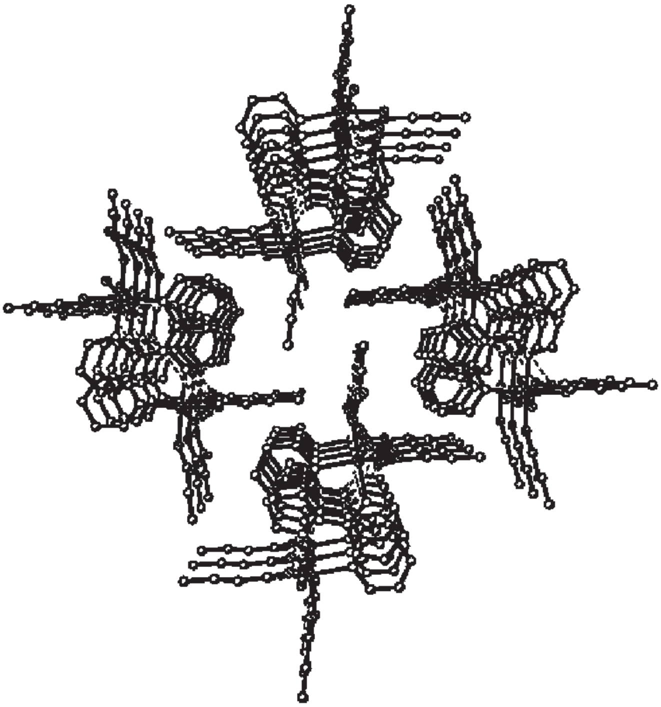

Figure 8. Crystal packing diagram of complex **3** viewed down *a*-axis. Hydrogen atoms are omitted for clarity.

110–130°C for **3**), mainly due to the release of one water molecule per formula unit. The observed weight loss (4.50% **1**; 4.58% **2**; 4.25% **3**) is close to the calculated one (4.26%, **1**; 4.56% **2**; 4.26% **3**). The temperatures for weight loss of hydration and coordinated water molecules are consistent with other compounds described in the literature, suggesting that the water molecules in **1** and **2** are hydration water and **3** is coordinated water.

Between 180 and 450°C the weight loss is noticeable for **1** and **2**, accompanying amassing of heat, corresponding to the decomposition and oxidation of α,β-unsaturated carboxylate and 2,2′-dipyridylamine. For **3**, in the temperature range of 180–400°C, DTA curve shows an exothermic peak at 316.3°C, and the complex underwent a large weight loss step. However, there is also an exothermic peak at 644.5°C, with a noticeable weight loss. The total observed weight loss and heating effects belong to 2,2′-dipyridylamine and α,β-unsaturated carboxylate groups together. The final product of **1**–**3** is CuO. The experimental residual percentage weights (obsd. 17.77% for **1**, 20.42% for **2** and 20.66% for **3**) at the end of the decomposition of the polymers are consistent with the calculated values of 25.65% for **1**, 28.19% for **2** and 18.79% for **3**. The analysis results showed the three complexes have no accurate melting point because of decomposition.

3.4. *Computational results and discussion*

Some atomic net charges are listed in table 4. Mulliken charges of the Cu change from +2 to 0.588*e* (complex **1**), 0.590*e* (complex **2**) and 0.558*e* (complex **3**) indicating the Cu charge has been decreased by the ligands. The net atomic charge of most acoordinated N and O atoms is negative, resulting in negative charge channels. These data show strong interaction between Cu and its coordinated atoms. In complex **3**, the total mulliken charge of H_2O is 0.077*e*, while the H_2O in complexes **1** and **2** is −0.027 and 0.001*e* respectively, confirming that H_2O coordinated to copper in complex **3**. In complexes **1** and **2**, the charge of zero indicates H_2O is free and not coordinated.

According to molecular orbital theory, frontier and nearby molecular orbitals are the most important factors to the activity. Larger differences in frontier orbitals give a

Table 4. Mulliken net atomic charge (*e*) for **1**–**3**.

Atom	Charge	Atom	Charge
Complex **1**			
Cu	0.588	N(1)	−0.616
N(2)	−0.560	N(3)	−0.699
O(1)	−0.520	O(2)	−0.548
O(3)	−0.574	O(4)	−0.792
C(1)	0.123	C(10)	0.131
H_2O	−0.027		
Complex **2**			
Cu	0.590	N(1)	−0.611
N(3)	−0.611	N(2)	−0.806
O(2)	−0.578	O(4)	−0.806
O(1)	−0.524	O(3)	−0.518
C(7)	0.122	C(16)	0.123
H_2O	0.001		
Complex **3**			
Cu	0.558	N(1)	−0.583
N(3)	−0.604	N(2)	−0.754
O(1)	−0.566	O(3)	−0.505
O(2)	−0.603	O(4)	−0.577
O(5)	−0.738	C(1)	0.150
C(10)	0.116	H_2O	0.077

Table 5. Frontier molecular orbital energies (eV).

Molecule	$E_{\mathrm{HOMO-2}}$	$E_{\mathrm{HOMO-1}}$	E_{HOMO}	E_{LUMO}	$E_{\mathrm{LUMO+1}}$	$E_{\mathrm{LUMO+2}}$	$\Delta E_{\mathrm{H \to L}}$
Complex **1**	−6.236	−5.940	−5.541	−2.027	−1.764	−1.312	3.514
Complex **2**	−6.342	−6.102	−5.788	−2.506	−1.696	−1.457	3.282
Complex **3**	−6.225	−6.078	−5.733	−1.592	1.360	−0.948	4.141

more stable structure [20]. ΔE ($\Delta E = E_{\mathrm{LUMO}} - E_{\mathrm{HOMO}}$) of complexes **1**, **2**, and **3** equals 3.514, 3.282 and 4.141 eV, all positive, showing the complexes are stable.

4. Conclusion

We have synthesized three new mononuclear complexes [Cu(CH$_2$=C(Me)CO$_2$)$_2$(dpa)] · H$_2$O (**1**), [Cu(CH$_2$=CHCO$_2$)$_2$(dpa)] · H$_2$O (**2**) and Cu(CH$_3$CH=CHCO$_2$)$_2$(dpa)(H$_2$O) (**3**) (dpa = 2,2′-dipyridylamine). The mononuclear units of the three complexes have strong hydrogen bonding between the amine N of dpa, carboxylate oxygen and aqua oxygen atom to form 1D double chains or a 2D network. The differences in **1**–**3** show the lattice water molecule and the arrangement of the neutral mononuclear units may tailor topology with different architectures using strong and weak non-covalent forces. A detailed crystal structure analysis of **2** revealed that the intermolecular hydrogen bonding is responsible for the significant supramolecular structural differences between **1** and **2**. In addition, we addressed molecular energies, stabilities and atomic charge, and the DFT calculations proved the water molecules coordinate to copper(II) in complex **3**, but are free in complexes **1** and **2**.

Supplementary data

Crystallographic data (excluding the structure factors) for the structure reported in this article have been deposited with the Cambridge Crystallographic Data Centre as supplementary publication no. CCDC-26289, CCDC-262892 and CCDC-262893 for **1**–**3**, respectively. Copies of the data can be obtained free of charge on application to CCDC, 12 Union Road, Cambridge CB2 1EZ, UK (Fax: (+44)1223-336-033; Email: deposit@ccdc.cam.ac.uk).

Acknowledgements

This work was supported by the National Natural Science Foundation of China (No. 20471048) and "TRAPOYT".

References

[1] G.R. Desiraju. *Nature*, **412**, 397 (2001).
[2] T. Steiner. *Angew. Chem. Int. Ed.*, **41**, 48 (2002).
[3] G.W. Gokel, A. Mukhopadhyay. *Chem. Soc. Rev.*, **30**, 274 (2001).
[4] O.R. Evans, W. Lin. *Acc. Chem. Res.*, **35**, 511 (2002).

[5] W. Kaim, B. Schwederski. *Bioinorganic Chemistry: Inorganic Elements in the Chemistry of Life*, Wiley, New York (1994).

[6] A. Camus, N. Marsich, A.M.M. Lanfredi, F. Ugozzoli, C. Massera. *Inorg. Chim. Acta*, **309**, 1 (2000).

[7] F.A. Cotton, L.M. Daniels, G.T. Jordan IV, C.A. Murillo. *J. Am. Chem. Soc.*, **119**, 10377 (1997).

[8] E.-C. Yang, M.-C. Cheng, M.-S. Tsai, S.-M. Peng. *J. Chem. Soc., Chem. Commun.*, **20**, 2377 (1994).

[9] L.-P. Wu, P. Field, T. Morrissey, C. Murphy, P. Nagle, B. Hathaway, C. Simmons, P. Thornton. *J. Chem. Soc., Dalton Trans.*, 3835 (1990).

[10] R. Lescouëzec, G. Marinescu, M.C. Muñoz, D. Luneau, M. Andruh, F. Lloret, J. Faus, M. Julve, J.A. Mata, R. Llusar. J. Cano. *New J. Chem.*, **25**, 1224 (2001).

[11] J.Y. Lu, V. Schauss. *Cryst. Eng. Comm.*, **4**(105), 623 (2002).

[12] D. Bose, S.H. Rahaman, G. Mostafa, R.D. Bailey Walsh, M.J. Zaworotko, B.K. Ghosh. *Polyhedron*, **23**, 545 (2004).

[13] T.J. Hurley, M.A. Robinson. *Inorg. Chem.*, **7**, 33 (1968).

[14] Y.Y. Wang, Q. Shi, Y.C. Gao, Q.Z. Shi. *Chinese Sci. Bull.*, **57**(5), 557 (1999).

[15] Y.Y. Wang, Q. Shi, Q.Z. Shi, Y.C. Gao. *Transition Met. Chem.*, **25**, 382 (2000).

[16] A.K. Vrkic, T. Taverner. *J. Chem. Soc., Dalton Trans.*, 198 (2004).

[17] Y.C. Gao, Y.Y. Wang, Q.Z. Shi. *Polyhedron*, **10**(16), 1893 (1991).

[18] K. Nakamoto. *Infrared and Raman Spectra of Inorganic and Coordination Compounds*, Wiley, New York (1978).

[19] W.R. McWhinnie. *Coord. Chem. Rev.*, **5**, 293 (1970).

[20] K.C. Zheng, Z.N. Chen. *Acta Phys.-Chim. Sinica* (*Chinese*), **15**(3), 204 (1999).